

10-20-2006

Search for the Standard Model Higgs Boson in the $p\bar{p} \rightarrow ZH \rightarrow \nu\bar{\nu}b\bar{b}$ Channel

V.M. Abazov

Joint Institute for Nuclear Research, Dubna, Russia

Kenneth A. Bloom

University of Nebraska - Lincoln, kbloom2@unl.edu

Gregory R. Snow

University of Nebraska-Lincoln, gsnow1@unl.edu

D0 Collaboration

Follow this and additional works at: <http://digitalcommons.unl.edu/physicsbloom>



Part of the [Physics Commons](#)

Abazov, V.M.; Bloom, Kenneth A.; Snow, Gregory R.; and Collaboration, D0, "Search for the Standard Model Higgs Boson in the $p\bar{p} \rightarrow ZH \rightarrow \nu\bar{\nu}b\bar{b}$ Channel" (2006). *Kenneth Bloom Publications*. 208.
<http://digitalcommons.unl.edu/physicsbloom/208>

This Article is brought to you for free and open access by the Research Papers in Physics and Astronomy at DigitalCommons@University of Nebraska - Lincoln. It has been accepted for inclusion in Kenneth Bloom Publications by an authorized administrator of DigitalCommons@University of Nebraska - Lincoln.

Search for the Standard Model Higgs Boson in the $p\bar{p} \rightarrow ZH \rightarrow \nu\bar{\nu}b\bar{b}$ Channel

V. M. Abazov,³⁶ B. Abbott,⁷⁶ M. Abolins,⁶⁶ B. S. Acharya,²⁹ M. Adams,⁵² T. Adams,⁵⁰ M. Agelou,¹⁸ J.-L. Agram,¹⁹ S. H. Ahn,³¹ M. Ahsan,⁶⁰ G. D. Alexeev,³⁶ G. Alkhalaf,⁴⁰ A. Alton,⁶⁵ G. Alverson,⁶⁴ G. A. Alves,² M. Anastasoiaie,³⁵ T. Andeen,⁵⁴ S. Anderson,⁴⁶ B. Andrieu,¹⁷ M. S. Anzels,⁵⁴ Y. Arnoud,¹⁴ M. Arov,⁵³ A. Askew,⁵⁰ B. Åsman,⁴¹ A. C. S. Assis Jesus,³ O. Atramentov,⁵⁸ C. Autermann,²¹ C. Avila,⁸ C. Ay,²⁴ F. Badaud,¹³ A. Baden,⁶² L. Bagby,⁵³ B. Baldin,⁵¹ D. V. Bandurin,⁶⁰ P. Banerjee,²⁹ S. Banerjee,²⁹ E. Barberis,⁶⁴ P. Bargassa,⁸¹ P. Baringer,⁵⁹ C. Barnes,⁴⁴ J. Barreto,² J. F. Bartlett,⁵¹ U. Bassler,¹⁷ D. Bauer,⁴⁴ A. Bean,⁵⁹ M. Begalli,³ M. Begel,⁷² C. Belanger-Champagne,⁵ L. Bellantoni,⁵¹ A. Bellavance,⁶⁸ J. A. Benitez,⁶⁶ S. B. Beri,²⁷ G. Bernardi,¹⁷ R. Bernhard,⁴² L. Berntzon,¹⁵ I. Bertram,⁴³ M. Besançon,¹⁸ R. Beuselinck,⁴⁴ V. A. Bezzubov,³⁹ P. C. Bhat,⁵¹ V. Bhatnagar,²⁷ M. Binder,²⁵ C. Biscarat,⁴³ K. M. Black,⁶³ I. Blackler,⁴⁴ G. Blazey,⁵³ F. Blekman,⁴⁴ S. Blessing,⁵⁰ D. Bloch,¹⁹ K. Bloom,⁶⁸ U. Blumenschein,²³ A. Boehnlein,⁵¹ O. Boeriu,⁵⁶ T. A. Bolton,⁶⁰ G. Borissov,⁴³ K. Bos,³⁴ T. Bose,⁷⁸ A. Brandt,⁷⁹ R. Brock,⁶⁶ G. Brooijmans,⁷¹ A. Bross,⁵¹ D. Brown,⁷⁹ N. J. Buchanan,⁵⁰ D. Buchholz,⁵⁴ M. Buehler,⁸² V. Buescher,²³ S. Burdin,⁵¹ S. Burke,⁴⁶ T. H. Burnett,⁸³ E. Busato,¹⁷ C. P. Buszello,⁴⁴ J. M. Butler,⁶³ P. Calfayan,²⁵ S. Calvet,¹⁵ J. Cammin,⁷² S. Caron,³⁴ W. Carvalho,³ B. C. K. Casey,⁷⁸ N. M. Cason,⁵⁶ H. Castilla-Valdez,³³ S. Chakrabarti,²⁹ D. Chakraborty,⁵³ K. M. Chan,⁷² A. Chandra,⁴⁹ D. Chapin,⁷⁸ F. Charles,¹⁹ E. Cheu,⁴⁶ F. Chevallier,¹⁴ D. K. Cho,⁶³ S. Choi,³² B. Choudhary,²⁸ L. Christofek,⁵⁹ D. Claes,⁶⁸ B. Clément,¹⁹ C. Clément,⁴¹ Y. Coadou,⁵ M. Cooke,⁸¹ W. E. Cooper,⁵¹ D. Coppage,⁵⁹ M. Corcoran,⁸¹ M.-C. Cousinou,¹⁵ B. Cox,⁴⁵ S. Crépe-Renaudin,¹⁴ D. Cutts,⁷⁸ M. Cwiok,³⁰ H. da Motta,² A. Das,⁶³ M. Das,⁶¹ B. Davies,⁴³ G. Davies,⁴⁴ G. A. Davis,⁵⁴ K. De,⁷⁹ P. de Jong,³⁴ S. J. de Jong,³⁵ E. De La Cruz-Burelo,⁶⁵ C. De Oliveira Martins,³ J. D. Degenhardt,⁶⁵ F. Déliot,¹⁸ M. Demarteau,⁵¹ R. Demina,⁷² P. Demine,¹⁸ D. Denisov,⁵¹ S. P. Denisov,³⁹ S. Desai,⁷³ H. T. Diehl,⁵¹ M. Diesburg,⁵¹ M. Doidge,⁴³ A. Dominguez,⁶⁸ H. Dong,⁷³ L. V. Dudko,³⁸ L. Duflot,¹⁶ S. R. Dugad,²⁹ A. Duperrin,¹⁵ J. Dyer,⁶⁶ A. Dyshkant,⁵³ M. Eads,⁶⁸ D. Edmunds,⁶⁶ T. Edwards,⁴⁵ J. Ellison,⁴⁹ J. Elmsheuser,²⁵ V. D. Elvira,⁵¹ S. Eno,⁶² P. Ermolov,³⁸ J. Estrada,⁵¹ H. Evans,⁵⁵ A. Evdokimov,³⁷ V. N. Evdokimov,³⁹ S. N. Fatakia,⁶³ L. Feligioni,⁶³ A. V. Ferapontov,⁶⁰ T. Ferbel,⁷² F. Fiedler,²⁵ F. Filthaut,³⁵ W. Fisher,⁵¹ H. E. Fisk,⁵¹ I. Fleck,²³ M. Ford,⁴⁵ M. Fortner,⁵³ H. Fox,²³ S. Fu,⁵¹ S. Fuess,⁵¹ T. Gadfort,⁸³ C. F. Galea,³⁵ E. Gallas,⁵¹ E. Galyaev,⁵⁶ C. Garcia,⁷² A. Garcia-Bellido,⁸³ J. Gardner,⁵⁹ V. Gavrilov,³⁷ A. Gay,¹⁹ P. Gay,¹³ D. Gelé,¹⁹ R. Gelhaus,⁴⁹ C. E. Gerber,⁵² Y. Gershtein,⁵⁰ D. Gillberg,⁵ G. Ginter,⁷² N. Gollub,⁴¹ B. Gómez,⁸ A. Goussiou,⁵⁶ P. D. Grannis,⁷³ H. Greenlee,⁵¹ Z. D. Greenwood,⁶¹ E. M. Gregores,⁴ G. Grenier,²⁰ Ph. Gris,¹³ J.-F. Grivaz,¹⁶ S. Grünendahl,⁵¹ M. W. Grünewald,³⁰ F. Guo,⁷³ J. Guo,⁷³ G. Gutierrez,⁵¹ P. Gutierrez,⁷⁶ A. Haas,⁷¹ N. J. Hadley,⁶² P. Haefner,²⁵ S. Hagopian,⁵⁰ J. Haley,⁶⁹ I. Hall,⁷⁶ R. E. Hall,⁴⁸ L. Han,⁷ K. Hanagaki,⁵¹ K. Harder,⁶⁰ A. Harel,⁷² R. Harrington,⁶⁴ J. M. Hauptman,⁵⁸ R. Hauser,⁶⁶ J. Hays,⁵⁴ T. Hebbeker,²¹ D. Hedin,⁵³ J. G. Hegeman,³⁴ J. M. Heinmiller,⁵² A. P. Heinson,⁴⁹ U. Heintz,⁶³ C. Hensel,⁵⁹ G. Hesketh,⁶⁴ M. D. Hildreth,⁵⁶ R. Hirosky,⁸² J. D. Hobbs,⁷³ B. Hoeneisen,¹² H. Hoeth,²⁶ M. Hohlfield,¹⁶ S. J. Hong,³¹ R. Hooper,⁷⁸ P. Houben,³⁴ Y. Hu,⁷³ Z. Hubacek,¹⁰ V. Hynek,⁹ I. Iashvili,⁷⁰ R. Illingworth,⁵¹ A. S. Ito,⁵¹ S. Jabeen,⁶³ M. Jaffré,¹⁶ S. Jain,⁷⁶ K. Jakobs,²³ C. Jarvis,⁶² A. Jenkins,⁴⁴ R. Jesik,⁴⁴ K. Johns,⁴⁶ C. Johnson,⁷¹ M. Johnson,⁵¹ A. Jonckheere,⁵¹ P. Jonsson,⁴⁴ A. Juste,⁵¹ D. Käfer,²¹ S. Kahn,⁷⁴ E. Kajfasz,¹⁵ A. M. Kalinin,³⁶ J. M. Kalk,⁶¹ J. R. Kalk,⁶⁶ S. Kappler,²¹ D. Karmanov,³⁸ J. Kasper,⁶³ P. Kasper,⁵¹ I. Katsanos,⁷¹ D. Kau,⁵⁰ R. Kaur,²⁷ R. Kehoe,⁸⁰ S. Kermiche,¹⁵ S. Kesisoglou,⁷⁸ N. Khalatyan,⁶³ A. Khanov,⁷⁷ A. Kharchilava,⁷⁰ Y. M. Kharzhev,³⁶ D. Khatidze,⁷¹ H. Kim,⁷⁹ T. J. Kim,³¹ M. H. Kirby,³⁵ B. Klima,⁵¹ J. M. Kohli,²⁷ J.-P. Konrath,²³ M. Kopal,⁷⁶ V. M. Korablev,³⁹ J. Kotcher,⁷⁴ B. Kothari,⁷¹ A. Koubarovsky,³⁸ A. V. Kozelov,³⁹ J. Kozminski,⁶⁶ D. Krop,⁵⁵ A. Kryemadhi,⁸² T. Kuhl,²⁴ A. Kumar,⁷⁰ S. Kunori,⁶² A. Kupco,¹¹ T. Kurča,^{20,*} J. Kvita,⁹ S. Lager,⁴¹ S. Lammers,⁷¹ G. Landsberg,⁷⁸ J. Lazoflores,⁵⁰ A.-C. Le Bihan,¹⁹ P. Lebrun,²⁰ W. M. Lee,⁵³ A. Leflat,³⁸ F. Lehner,⁴² V. Lesne,¹³ J. Leveque,⁴⁶ P. Lewis,⁴⁴ J. Li,⁷⁹ Q. Z. Li,⁵¹ J. G. R. Lima,⁵³ D. Lincoln,⁵¹ J. Linnemann,⁶⁶ V. V. Lipaev,³⁹ R. Lipton,⁵¹ Z. Liu,⁵ L. Lobo,⁴⁴ A. Lobodenko,⁴⁰ M. Lokajicek,¹¹ A. Lounis,¹⁹ P. Love,⁴³ H. J. Lubatti,⁸³ M. Lynker,⁵⁶ A. L. Lyon,⁵¹ A. K. A. Maciel,² R. J. Madaras,⁴⁷ P. Mättig,²⁶ C. Magass,²¹ A. Magerkurth,⁶⁵ A.-M. Magnan,¹⁴ N. Makovec,¹⁶ P. K. Mal,⁵⁶ H. B. Malbouisson,³ S. Malik,⁶⁸ V. L. Malyshev,³⁶ H. S. Mao,⁶ Y. Maravin,⁶⁰ M. Martens,⁵¹ S. E. K. Mattingly,⁷⁸ R. McCarthy,⁷³ D. Meder,²⁴ A. Melnitchouk,⁶⁷ A. Mendes,¹⁵ L. Mendoza,⁸ M. Merkin,³⁸ K. W. Merritt,⁵¹ A. Meyer,²¹ J. Meyer,²² M. Michaut,¹⁸ H. Miettinen,⁸¹ T. Millet,²⁰ J. Mitrevski,⁷¹ J. Molina,³ N. K. Mondal,²⁹ J. Monk,⁴⁵ R. W. Moore,⁵ T. Mouluk,⁵⁹ G. S. Muanza,¹⁶ M. Mulders,⁵¹ M. Mulhearn,⁷¹ L. Mundim,³ Y. D. Mutaf,⁷³ E. Nagy,¹⁵ M. Naimuddin,²⁸ M. Narain,⁶³ N. A. Naumann,³⁵ H. A. Neal,⁶⁵ J. P. Negret,⁸ S. Nelson,⁵⁰ P. Neustroev,⁴⁰ C. Noeding,²³ A. Nomerotski,⁵¹ S. F. Novaes,⁴ T. Nunnemann,²⁵ V. O'Dell,⁵¹ D. C. O'Neil,⁵ G. Obrant,⁴⁰ V. Oguri,³ N. Oliveira,³ N. Oshima,⁵¹ R. Otec,¹⁰ G. J. Otero y Garzón,⁵² M. Owen,⁴⁵ P. Padley,⁸¹ N. Parashar,⁵⁷ S.-J. Park,⁷²

S. K. Park,³¹ J. Parsons,⁷¹ R. Partridge,⁷⁸ N. Parua,⁷³ A. Patwa,⁷⁴ G. Pawloski,⁸¹ P. M. Perea,⁴⁹ E. Perez,¹⁸ K. Peters,⁴⁵ P. Pétroff,¹⁶ M. Petteni,⁴⁴ R. Piegaia,¹ M.-A. Pleier,²² P. L. M. Podesta-Lerma,³³ V. M. Podstavkov,⁵¹ Y. Pogorelov,⁵⁶ M.-E. Pol,² A. Pompoš,⁷⁶ B. G. Pope,⁶⁶ A. V. Popov,³⁹ W. L. Prado da Silva,³ H. B. Prosper,⁵⁰ S. Protopopescu,⁷⁴ J. Qian,⁶⁵ A. Quadt,²² B. Quinn,⁶⁷ K. J. Rani,²⁹ K. Ranjan,²⁸ P. N. Ratoff,⁴³ P. Renkel,⁸⁰ S. Reucroft,⁶⁴ M. Rijssenbeek,⁷³ I. Ripp-Baudot,¹⁹ F. Rizatdinova,⁷⁷ S. Robinson,⁴⁴ R. F. Rodrigues,³ C. Royon,¹⁸ P. Rubinov,⁵¹ R. Ruchti,⁵⁶ V. I. Rud,³⁸ G. Sajot,¹⁴ A. Sánchez-Hernández,³³ M. P. Sanders,⁶² A. Santoro,³ G. Savage,⁵¹ L. Sawyer,⁶¹ T. Scanlon,⁴⁴ D. Schaile,²⁵ R. D. Schamberger,⁷³ Y. Scheglov,⁴⁰ H. Schellman,⁵⁴ P. Schieferdecker,²⁵ C. Schmitt,²⁶ C. Schwanenberger,⁴⁵ A. Schwartzman,⁶⁹ R. Schwienhorst,⁶⁶ S. Sengupta,⁵⁰ H. Severini,⁷⁶ E. Shabalina,⁵² M. Shamim,⁶⁰ V. Shary,¹⁸ A. A. Shchukin,³⁹ W. D. Shephard,⁵⁶ R. K. Shivpuri,²⁸ D. Shpakov,⁵¹ V. Siccaldi,¹⁹ R. A. Sidwell,⁶⁰ V. Simak,¹⁰ V. Sirotenko,⁵¹ P. Skubic,⁷⁶ P. Slattey,⁷² R. P. Smith,⁵¹ G. R. Snow,⁶⁸ J. Snow,⁷⁵ S. Snyder,⁷⁴ S. Söldner-Rembold,⁴⁵ X. Song,⁵³ L. Sonnenschein,¹⁷ A. Sopczak,⁴³ M. Sosebee,⁷⁹ K. Soustruznik,⁹ M. Souza,² B. Spurlock,⁷⁹ J. Stark,¹⁴ J. Steele,⁶¹ V. Stolin,³⁷ A. Stone,⁵² D. A. Stoyanova,³⁹ J. Strandberg,⁴¹ M. A. Strang,⁷⁰ M. Strauss,⁷⁶ R. Ströhmer,²⁵ D. Strom,⁵⁴ M. Strovink,⁴⁷ L. Stutte,⁵¹ S. Sumowidagdo,⁵⁰ A. Sznajder,³ M. Talby,¹⁵ P. Tamburello,⁴⁶ W. Taylor,⁵ P. Telford,⁴⁵ J. Temple,⁴⁶ B. Tiller,²⁵ M. Titov,²³ V. V. Tokmenin,³⁶ M. Tomoto,⁵¹ T. Toole,⁶² I. Torchiani,²³ S. Towers,⁴³ T. Trefzger,²⁴ S. Trincaz-Duvoid,¹⁷ D. Tsybychev,⁷³ B. Tuchming,¹⁸ C. Tully,⁶⁹ A. S. Turcot,⁴⁵ P. M. Tuts,⁷¹ R. Unalan,⁶⁶ L. Uvarov,⁴⁰ S. Uvarov,⁴⁰ S. Uzunyan,⁵³ B. Vachon,⁵ P. J. van den Berg,³⁴ R. Van Kooten,⁵⁵ W. M. van Leeuwen,³⁴ N. Varelas,⁵² E. W. Varnes,⁴⁶ A. Vartapetian,⁷⁹ I. A. Vasilyev,³⁹ M. Vaupel,²⁶ P. Verdier,²⁰ L. S. Vertogradov,³⁶ M. Verzocchi,⁵¹ F. Villeneuve-Seguier,⁴⁴ P. Vint,⁴⁴ J.-R. Vlimant,¹⁷ E. Von Toerne,⁶⁰ M. Voutilainen,^{68,†} M. Vreeswijk,³⁴ H. D. Wahl,⁵⁰ L. Wang,⁶² J. Warchol,⁵⁶ G. Watts,⁸³ M. Wayne,⁵⁶ M. Weber,⁵¹ H. Weerts,⁶⁶ N. Wermes,²² M. Wetstein,⁶² A. White,⁷⁹ D. Wicke,²⁶ G. W. Wilson,⁵⁹ S. J. Wimpenny,⁴⁹ M. Wobisch,⁵¹ J. Womersley,⁵¹ D. R. Wood,⁶⁴ T. R. Wyatt,⁴⁵ Y. Xie,⁷⁸ N. Xuan,⁵⁶ S. Yacoob,⁵⁴ R. Yamada,⁵¹ M. Yan,⁶² T. Yasuda,⁵¹ Y. A. Yatsunenko,³⁶ K. Yip,⁷⁴ H. D. Yoo,⁷⁸ S. W. Youn,⁵⁴ C. Yu,¹⁴ J. Yu,⁷⁹ A. Yurkewicz,⁷³ A. Zatserklyaniy,⁵³ C. Zeitnitz,²⁶ D. Zhang,⁵¹ T. Zhao,⁸³ B. Zhou,⁶⁵ J. Zhu,⁷³ M. Zielinski,⁷² D. Zieminska,⁵⁵ A. Zieminski,⁵⁵ V. Zutshi,⁵³ and E. G. Zverev³⁸

(D0 Collaboration)

¹Universidad de Buenos Aires, Buenos Aires, Argentina

²LAFEX, Centro Brasileiro de Pesquisas Físicas, Rio de Janeiro, Brazil

³Universidade do Estado do Rio de Janeiro, Rio de Janeiro, Brazil

⁴Instituto de Física Teórica, Universidade Estadual Paulista, São Paulo, Brazil

⁵University of Alberta, Edmonton, Alberta, Canada;

Simon Fraser University, Burnaby, British Columbia, Canada;

York University, Toronto, Ontario, Canada;

and McGill University, Montreal, Quebec, Canada

⁶Institute of High Energy Physics, Beijing, People's Republic of China

⁷University of Science and Technology of China, Hefei, People's Republic of China

⁸Universidad de los Andes, Bogotá, Colombia

⁹Center for Particle Physics, Charles University, Prague, Czech Republic

¹⁰Czech Technical University, Prague, Czech Republic

¹¹Center for Particle Physics, Institute of Physics, Academy of Sciences of the Czech Republic, Prague, Czech Republic

¹²Universidad San Francisco de Quito, Quito, Ecuador

¹³Laboratoire de Physique Corpusculaire, IN2P3-CNRS, Université Blaise Pascal, Clermont-Ferrand, France

¹⁴Laboratoire de Physique Subatomique et de Cosmologie, IN2P3-CNRS, Université de Grenoble 1, Grenoble, France

¹⁵CPPM, IN2P3-CNRS, Université de la Méditerranée, Marseille, France

¹⁶IN2P3-CNRS, Laboratoire de l'Accélérateur Linéaire, Orsay, France

¹⁷LPNHE, IN2P3-CNRS, Universités Paris VI and VII, Paris, France

¹⁸DAPNIA/Service de Physique des Particules, CEA, Saclay, France

¹⁹IPHC, IN2P3-CNRS, Université Louis Pasteur, Strasbourg, France,

and Université de Haute Alsace, Mulhouse, France

²⁰Institut de Physique Nucléaire de Lyon, IN2P3-CNRS, Université Claude Bernard, Villeurbanne, France

²¹III. Physikalisches Institut A, RWTH Aachen, Aachen, Germany

²²Physikalisches Institut, Universität Bonn, Bonn, Germany

²³Physikalisches Institut, Universität Freiburg, Freiburg, Germany

²⁴Institut für Physik, Universität Mainz, Mainz, Germany

²⁵Ludwig-Maximilians-Universität München, München, Germany

²⁶Fachbereich Physik, University of Wuppertal, Wuppertal, Germany

- ²⁷Panjab University, Chandigarh, India
²⁸Delhi University, Delhi, India
²⁹Tata Institute of Fundamental Research, Mumbai, India
³⁰University College Dublin, Dublin, Ireland
³¹Korea Detector Laboratory, Korea University, Seoul, Korea
³²SungKyunKwan University, Suwon, Korea
³³CINVESTAV, Mexico City, Mexico
³⁴FOM-Institute NIKHEF and University of Amsterdam/NIKHEF, Amsterdam, The Netherlands
³⁵Radboud University Nijmegen/NIKHEF, Nijmegen, The Netherlands
³⁶Joint Institute for Nuclear Research, Dubna, Russia
³⁷Institute for Theoretical and Experimental Physics, Moscow, Russia
³⁸Moscow State University, Moscow, Russia
³⁹Institute for High Energy Physics, Protvino, Russia
⁴⁰Petersburg Nuclear Physics Institute, St. Petersburg, Russia
⁴¹Lund University, Lund, Sweden; Royal Institute of Technology and Stockholm University, Stockholm, Sweden;
Uppsala University, Uppsala, Sweden
⁴²Physik Institut der Universität Zürich, Zürich, Switzerland
⁴³Lancaster University, Lancaster, United Kingdom
⁴⁴Imperial College, London, United Kingdom
⁴⁵University of Manchester, Manchester, United Kingdom
⁴⁶University of Arizona, Tucson, Arizona 85721, USA
⁴⁷Lawrence Berkeley National Laboratory and University of California, Berkeley, California 94720, USA
⁴⁸California State University, Fresno, California 93740, USA
⁴⁹University of California, Riverside, California 92521, USA
⁵⁰Florida State University, Tallahassee, Florida 32306, USA
⁵¹Fermi National Accelerator Laboratory, Batavia, Illinois 60510, USA
⁵²University of Illinois at Chicago, Chicago, Illinois 60607, USA
⁵³Northern Illinois University, DeKalb, Illinois 60115, USA
⁵⁴Northwestern University, Evanston, Illinois 60208, USA
⁵⁵Indiana University, Bloomington, Indiana 47405, USA
⁵⁶University of Notre Dame, Notre Dame, Indiana 46556, USA
⁵⁷Purdue University Calumet, Hammond, Indiana 46323, USA
⁵⁸Iowa State University, Ames, Iowa 50011, USA
⁵⁹University of Kansas, Lawrence, Kansas 66045, USA
⁶⁰Kansas State University, Manhattan, Kansas 66506, USA
⁶¹Louisiana Tech University, Ruston, Louisiana 71272, USA
⁶²University of Maryland, College Park, Maryland 20742, USA
⁶³Boston University, Boston, Massachusetts 02215, USA
⁶⁴Northeastern University, Boston, Massachusetts 02115, USA
⁶⁵University of Michigan, Ann Arbor, Michigan 48109, USA
⁶⁶Michigan State University, East Lansing, Michigan 48824, USA
⁶⁷University of Mississippi, University, Mississippi 38677, USA
⁶⁸University of Nebraska, Lincoln, Nebraska 68588, USA
⁶⁹Princeton University, Princeton, New Jersey 08544, USA
⁷⁰State University of New York, Buffalo, New York 14260, USA
⁷¹Columbia University, New York, New York 10027, USA
⁷²University of Rochester, Rochester, New York 14627, USA
⁷³State University of New York, Stony Brook, New York 11794, USA
⁷⁴Brookhaven National Laboratory, Upton, New York 11973, USA
⁷⁵Langston University, Langston, Oklahoma 73050, USA
⁷⁶University of Oklahoma, Norman, Oklahoma 73019, USA
⁷⁷Oklahoma State University, Stillwater, Oklahoma 74078, USA
⁷⁸Brown University, Providence, Rhode Island 02912, USA
⁷⁹University of Texas, Arlington, Texas 76019, USA
⁸⁰Southern Methodist University, Dallas, Texas 75275, USA
⁸¹Rice University, Houston, Texas 77005, USA
⁸²University of Virginia, Charlottesville, Virginia 22901, USA
⁸³University of Washington, Seattle, Washington 98195, USA

(Received 17 July 2006; published 20 October 2006)

We report a search for the standard model (SM) Higgs boson based on data collected by the D0 experiment at the Fermilab Tevatron Collider, corresponding to an integrated luminosity of 260 pb^{-1} . We study events with missing transverse energy and two acoplanar b jets, which provide sensitivity to the ZH production cross section in the $\nu\bar{\nu}b\bar{b}$ channel, and to WH production when the lepton from the $W \rightarrow \ell\nu$ decay is undetected. The data are consistent with the SM background expectation, and we set 95% C.L. upper limits on $\sigma(p\bar{p} \rightarrow ZH/WH) \times B(H \rightarrow b\bar{b})$ from 3.4/8.3 to 2.5/6.3 pb, for Higgs-boson masses between 105 and 135 GeV.

DOI: 10.1103/PhysRevLett.97.161803

PACS numbers: 14.80.Bn, 13.85.Ni, 13.85.Qk, 13.85.Rm

In the standard model (SM), the Higgs boson (H) responsible for electroweak symmetry breaking has yet to be observed. The experiments at the CERN e^+e^- Collider (LEP) provide lower limits on its mass, $m_H > 114.4 \text{ GeV}$, while electroweak global fits favor a light Higgs boson, $m_H < 207 \text{ GeV}$ at 95% C.L. [1]. If it exists, the Higgs boson could be observed at the Fermilab Tevatron Collider (center of mass energy $\sqrt{s} = 1.96 \text{ TeV}$) by combining different analysis channels from both the D0 and CDF experiments [2,3].

We present a search for a SM Higgs boson with m_H between 105 and 135 GeV, in the final state with missing transverse energy (\cancel{E}_T) and two or three jets, in which one or two jets are identified (“tagged”) as b jets. This final state is sensitive to Higgs bosons produced in the $p\bar{p} \rightarrow ZH \rightarrow \nu\bar{\nu}b\bar{b}$ channel, which is particularly promising because of the expected large $Z \rightarrow \nu\bar{\nu}$ and $H \rightarrow b\bar{b}$ branching fractions. The product of cross section (σ) and branching fraction (B) is predicted to be about 0.01 pb for a 115 GeV Higgs boson, which is comparable to that for $WH \rightarrow l\nu b\bar{b}$ [4].

The chosen final state also has sensitivity to WH production since the charged lepton from W decay can be undetected or not identified properly ($l\nu b\bar{b}$ channel). Searches for WH production have been performed previously by relying on the identification of the electron or the muon from leptonic W decay [5,6].

There are two main sources of background to this final state: (i) the “physics” backgrounds Z + jets, W + jets, electroweak diboson production (WZ and ZZ), and top quark production with undetected leptons or jets, and (ii) a large instrumental background caused by multijet events with mismeasured jet energies that is difficult to simulate. In the ZH or WH processes, since the two b jets are boosted along the Higgs-momentum direction, they are not back-to-back in azimuthal angle (φ), in contrast to the dominant dijet background. Our search is based on an integrated luminosity of 260 pb^{-1} accumulated with a dedicated trigger designed to select events with significant \cancel{E}_T and with jets that are not back to back.

The D0 tracking system consists of a silicon microstrip tracker (SMT) and a central fiber tracker (CFT), both located within a 2 T superconducting solenoidal magnet [7], with tracking and vertexing at pseudorapidities $|\eta| < 3$ and $|\eta| < 2.5$, respectively, where $\eta = -\ln[\tan(\theta/2)]$ and θ is the polar angle. A liquid-argon and uranium calorime-

ter has a central section (CC) covering $|\eta|$ up to ≈ 1.1 , and two end calorimeters (EC) that extend coverage to $|\eta| \approx 4.2$ [8]. An outer muon system, at $|\eta| < 2$, consists of a layer of tracking detectors and scintillation trigger counters in front of 1.8 T toroids, followed by two similar layers after the toroids.

To estimate the number of expected events, the signal (ZH , WH), $t\bar{t}$, and diboson production is simulated with PYTHIA [9]. For W and Z events with two or more jets we use ALPGEN [10], and for single top simulation we use COMPHEP [11]. The samples generated by COMPHEP and ALPGEN are passed through PYTHIA for showering and hadronization. The cross sections for the ALPGEN samples are normalized to next-to-leading-order calculations [12]. All the samples are processed through D0 detector simulation based on GEANT [13], and D0 reconstruction software. Trigger efficiencies measured in data are applied to correct the simulated events.

Event selection requires two or three jets reconstructed with the “iterative-midpoint-Run-II” cone algorithm, with $p_T > 20 \text{ GeV}$, $|\eta| < 2.5$, and a cone radius of $\Delta R = \sqrt{(\Delta\eta)^2 + (\Delta\varphi)^2} < 0.5$. Jets are required to pass quality criteria designed to reject noise and suppress electron or photon-induced energy depositions, and jet energies are corrected to the particle level using jet energy calibration and resolution factors determined from photon + jet events. Corrections depend on the p_T and η of the jet and are typically 30%. Jet energy resolution varies from 20% to 10% for p_T between 40 and 150 GeV.

The primary vertex has to be within $\pm 35 \text{ cm}$ of the longitudinal (z) center of the detector, and at least two “taggable” jets that pass the above requirements must be present for the event to be included in our final sample (a jet is defined taggable if it contains within its cone at least two tracks satisfying strict quality criteria, one with $p_T > 1 \text{ GeV}$, and another with $p_T > 0.5 \text{ GeV}$). The average fraction of taggable jets is measured using $W(\rightarrow \mu\nu)$ + jets data, and is $(86 \pm 1)\%$ per jet. This fraction, which is a function of η and p_T of the jet, and of the z coordinate of the primary vertex, is used to correct the simulated jets.

We then require: (i) $\cancel{E}_T > 50 \text{ GeV}$, where \cancel{E}_T is calculated from the position and energy of the calorimeter cells, (ii) the azimuthal angle between the two highest p_T (leading) jets to be less than 165° , and (iii) no isolated electrons or muons, in order to suppress multijet background and

$W(\rightarrow e\nu, \mu\nu) + \text{jet}$ and $Z(\rightarrow ee, \mu\mu) + \text{jet}$ events. For the rejection of $t\bar{t}$ background, we require the scalar sum H_T of the p_T of the jets to be less than 240 GeV. To further reduce instrumental background induced by mismeasurement of jet energy, which produces abnormal \cancel{E}_T , we define $\min\Delta\varphi(\vec{\cancel{E}}_T, \text{jets})$ as the minimum difference in φ between the direction of $\vec{\cancel{E}}_T$ and any of the jets, $\cancel{H}_T \equiv |\sum_{i=1}^{n_{\text{jet}}} \vec{p}_T|$ as the magnitude of the vector sum of the \vec{p}_T of the jets, $\vec{P}_T^{\text{trk}} \equiv -\sum_{i=1}^{n_{\text{trk}}} \vec{p}_T$ as opposite vector sum of the \vec{p}_T of all tracks, $\Delta\varphi(\vec{\cancel{E}}_T, \vec{P}_T^{\text{trk}})$ as the difference in φ between the direction of $\vec{\cancel{E}}_T$ and \vec{P}_T^{trk} , and $A(\vec{\cancel{E}}_T, \cancel{H}_T) \equiv (\cancel{E}_T - \cancel{H}_T)/(\cancel{E}_T + \cancel{H}_T)$ as the asymmetry between $\vec{\cancel{E}}_T$ and \cancel{H}_T . The instrumental background is significantly reduced by requiring: \cancel{E}_T (in GeV) $> 80 - 40 \times \min\Delta\varphi(\vec{\cancel{E}}_T, \text{jet})$, $|\vec{P}_T^{\text{trk}}| > 20$ GeV, $\Delta\varphi(\vec{\cancel{E}}_T, \vec{P}_T^{\text{trk}}) < \frac{\pi}{2}$, and $-0.1 < A(\vec{\cancel{E}}_T, \cancel{H}_T) < 0.2$. All these requirements define the signal region.

$W(\rightarrow \mu\nu) + \text{jets}$ data are used to confirm that the above variables are well modeled. The instrumental background is then estimated from the data using the signal and a “sideband” region, which is defined by requiring all above selections, except for the requirement $\Delta\varphi(\vec{\cancel{E}}_T, \vec{P}_T^{\text{trk}}) > \frac{\pi}{2}$. The distribution in the simulated instrumental background generated by PYTHIA gives a qualitative description of this background. This indicates that we are correctly identifying the background source, and we therefore model it using sideband data to avoid uncertainty from the difficult simulation of instrumental background. The physics backgrounds passing the final selection tend to be distributed around $\Delta\varphi(\vec{\cancel{E}}_T, \vec{P}_T^{\text{trk}}) \sim 0$, while the instrumental background is distributed similarly in the sideband and in the signal region due to mismeasurement of jet energy or of charged tracks.

Figure 1 shows the $A(\vec{\cancel{E}}_T, \cancel{H}_T)$ distribution in the signal region. The amount of physics background in the signal region is estimated using the simulation, and parametrized by a triple Gaussian (TG) function, shown as a dashed line in Fig. 1. The contribution not described by this parametrization is considered to be the instrumental background, and is modeled with a polynomial function tested through a fit to the data in the sideband region. The physics background contributes about 15% of the events in the sideband region and is included in the model of instrumental background.

The sum of the absolutely normalized TG parametrization and of the polynomial function is then fitted to the data in the signal region, as shown in Fig. 1. (Before b tagging, the Higgs signal is negligible.) The instrumental background in the signal region amounts to 696 ± 91 events, while the physics background amounts to 2520 ± 330 events. Since our search requires good modeling of \cancel{E}_T , we show in Fig. 2 the \cancel{E}_T distribution after all requirements, excepting b tagging. The data are well described by the

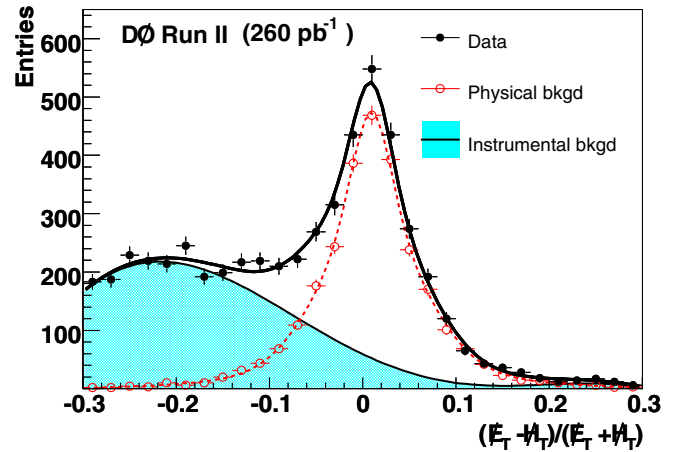


FIG. 1 (color online). Asymmetry distribution $A(\vec{\cancel{E}}_T, \cancel{H}_T)$ in the signal region, prior to the imposition of the requirement on $A(\vec{\cancel{E}}_T, \cancel{H}_T)$. The data are described by the sum of the physics background, modeled by a triple Gaussian, and the instrumental background modeled by a polynomial function.

sum of the simulation of $Z/W + jj/b\bar{b}$ and the estimated contribution from instrumental background. Top-pair and single top production represent negligible contributions before requiring b tagging.

To select b jets, we apply a b -tagging algorithm that uses a jet lifetime probability (JLIP) computed from the tracks associated with the jet. A small probability corresponds to jets having tracks with a large impact parameter that characterize b -hadron decay. We use two samples for our search: one that requires the two leading jets to pass the b -tagging condition (double b -tagged sample, or DT sample); the other requires exactly one jet to pass the b -tagging condition, and does not accept events from the DT sample (exclusive single b -tagged sample, or ST sample). The requirements on the lifetime probability are defined by optimizing the sensitivity to Higgs signal. In the DT sample,

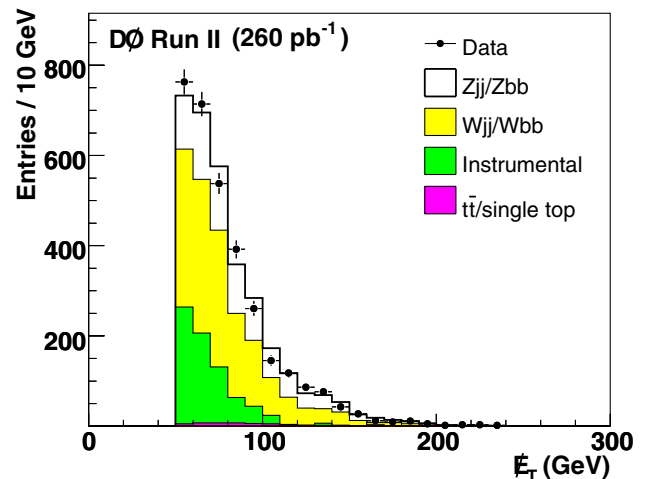


FIG. 2 (color online). \cancel{E}_T distribution after all selections except b tagging.

TABLE I. Number of expected signal (for $m_H = 115$ GeV), background, and observed events (obs.) before b tagging, after inclusive (IST), and exclusive (ST) single b tagging, and after double b tagging (DT). Before b tagging, the expected background is by construction equal to the observed events (see text on the background determination). The number of events after the ± 1.5 standard deviation (s.d.) mass window requirement are given in parenthesis. The average errors on these numbers are 18% (19%) for the ST (DT) sample.

	$\cancel{E}_T + 2, 3$ jets	$\cancel{E}_T + 2, 3$ jets IST	$\cancel{E}_T + 2, 3$ jets ST	$\cancel{E}_T + 2, 3$ jets DT
ZH	0.71	0.62	0.26 (0.20)	0.24 (0.21)
WH	0.54	0.47	0.20 (0.15)	0.18 (0.15)
Zjj	843	93.3	7.9 (2.6)	1.4 (0.5)
Wjj	1600	260	36.1 (13.6)	4.2 (1.5)
Zbb	13.1	11.3	4.7 (1.6)	4.1 (1.4)
Wbb	12.4	10.5	4.4 (1.4)	3.6 (1.1)
$t\bar{t}/tb/tqb$	42.3	33.6	15.3 (5.6)	9.0 (3.0)
WZ/ZZ	7.3	3.4	1.1 (0.71)	0.9 (0.6)
Instrumental	696	143	25.0 (8.4)	3.9 (1.3)
Total expectation	\equiv obs.	555	94.5 (34.0)	27.0 (9.4)
Observed events	3210	592	106 (33)	25 (11)

we require $JLIP < 1\%$ for the leading jet and $< 4\%$ for the second-leading jet. In the ST sample we require a more stringent $JLIP < 0.1\%$. The average b -tagging efficiency is $\approx 50\%$ (40%, 30%) for $JLIP < 4\%$ (1%, 0.1%). The relative uncertainty on the b -tagging efficiency is 7% per jet. The mistag rate is defined as the fraction of light-quark jets tagged as b jets, and its average value is approximately the value of the $JLIP$ requirement. For the instrumental background, we estimate the mistag rate from data in the sideband region, and extrapolate it into the signal region. Table I lists the number of ZH and WH signal, background, and observed events for each b -tag requirement, and also for the inclusive sample of events with at least one b -tagged jet with $JLIP < 4\%$ (to verify that the data are also well described by the simulation in another b -tagging

configuration). After the ST requirement, 106 events remain, while 94.5 ± 17.0 events are expected. In the DT sample, we observe 25 events, whereas 27.0 ± 5.1 are expected, and in the inclusive sample these numbers are 592 and 555 ± 70 events, respectively.

We estimate the systematic uncertainty due to trigger and jet reconstruction efficiency, jet energy calibration, jet resolution, b tagging, instrumental-background estimation, physics-background cross sections, and parton distribution functions by varying each source of uncertainty by ± 1 s.d. and repeating the analysis. The systematic uncertainties are estimated separately for the DT and ST samples. In total, we find a 19% (14%) uncertainty on signal acceptance and 19% (18%) uncertainty on the total background for the DT (ST) analysis. The dominant systematic uncertainties are due to b tagging and jet reconstruction and calibration. The uncertainty on the integrated luminosity is 6.5%.

We then search for an excess of events as a function of m_H by counting events in the dijet mass distribution within a ± 1.5 s.d. window around the reconstructed Higgs-boson mass peak, e.g., ± 25.2 GeV for $m_H = 115$ GeV. No excess over the SM background is found in the data, as can be seen for the DT dijet mass distribution in Fig. 3, in which the expected ZH signal for $m_H = 115$ GeV is also shown. The acceptance for ZH (WH) events is 1.04% (0.43%) for $m_H = 115$ GeV. We thus set 95% C.L. upper limits on

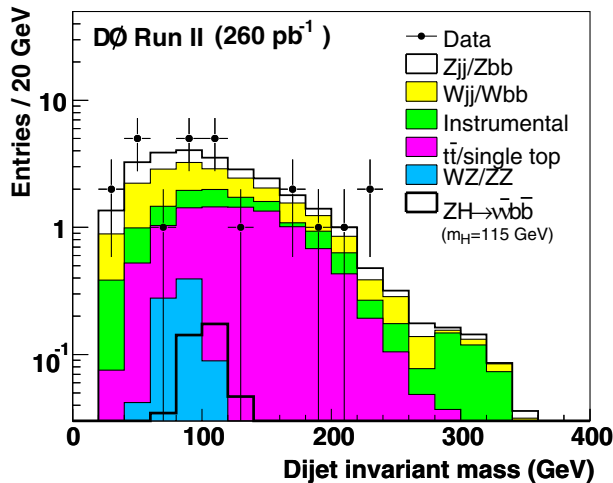


FIG. 3 (color online). Dijet invariant mass distribution in the DT sample. The expectation originating from ZH production with $m_H = 115$ GeV is also shown.

TABLE II. Expected/observed 95% C.L. limits on $\sigma(p\bar{p} \rightarrow ZH) \times B(H \rightarrow b\bar{b})$ in pb, as a function of m_H .

Higgs mass (GeV)	105	115	125	135
ST	7.7/8.2	6.8/6.8	6.0/7.3	5.4/7.5
DT	3.3/4.2	2.8/3.6	2.5/2.8	2.2/2.2
ST + DT	3.1/3.4	2.7/3.2	2.4/2.9	2.1/2.5

TABLE III. Expected/observed 95% C.L. limits on $\sigma(p\bar{p} \rightarrow WH) \times B(H \rightarrow b\bar{b})$ in pb, as a function of m_H .

Higgs mass (GeV)	105	115	125	135
ST	18.5/17.6	15.9/16.9	14.9/18.9	12.4/18.5
DT	8.0/9.6	6.6/8.1	6.3/7.1	5.3/5.3
ST + DT	7.6/8.3	6.3/7.5	6.0/7.4	5.0/6.3

$\sigma(p\bar{p} \rightarrow ZH) \times B(H \rightarrow b\bar{b})$ and $\sigma(p\bar{p} \rightarrow WH) \times B(H \rightarrow b\bar{b})$, using a modified frequentist approach, the CL_S method [14]. In this method, the binned distributions are summed over the log-likelihood ratio test statistic. Systematic uncertainties are incorporated into the signal and background expectations using Gaussian sampling of individual uncertainties. For the limits obtained when combining the likelihoods of the ST and DT analyses, correlations between uncertainties are handled by varying simultaneously all identical sources. Limits are determined by scaling the signal expectations until the probability for the background-only hypothesis falls below 5% (95% C.L.). This translates into a cross-section limit for $\sigma(p\bar{p} \rightarrow ZH) \times B(H \rightarrow b\bar{b})$ of 3.2 pb and for $\sigma(p\bar{p} \rightarrow WH) \times B(H \rightarrow b\bar{b})$ of 7.5 pb, assuming $m_H = 115$ GeV. The limits for four Higgs-boson mass points (105, 115, 125, and 135 GeV) and for ST, DT, and the combined ST + DT results are summarized in Tables II and III. We set 95% C.L. upper limits from 3.4 to 2.5 pb on $\sigma(p\bar{p} \rightarrow ZH) \times B(H \rightarrow b\bar{b})$ for $m_H = 105$ –135 GeV (Fig. 4). The CDF Collaboration has published combined limits (ST + DT) with Tevatron Run I data, i.e., at $\sqrt{s} = 1.8$ TeV, of 7.8–7.4 pb for $m_H = 110$ –130 GeV [15].

In conclusion, we have performed a search for ZH and WH associated production in the $\cancel{E}_T + b$ jets channel using 260 pb^{-1} of data. We have studied the dijet mass spectrum

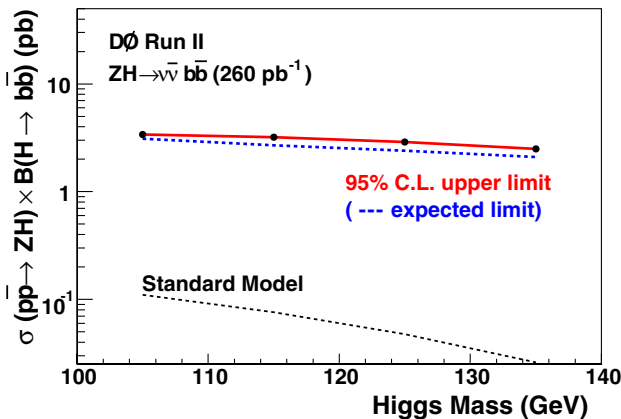


FIG. 4 (color online). 95% C.L. upper limit on $\sigma(p\bar{p} \rightarrow ZH) \times B(H \rightarrow b\bar{b})$ (and corresponding expected limit) for ZH production vs Higgs-boson mass, as derived from the ST + DT combination.

of the two leading jets with double and exclusive single b -tagged jets for Higgs-boson masses between 105 and 135 GeV. In the absence of signal, we have set upper limits on different Higgs-boson production channels or final states, and have combined them. The combined limits are between 3.4 to 2.5 pb (8.3 to 6.3 pb) on the cross section for ZH (WH) production multiplied by the branching fraction for $H \rightarrow b\bar{b}$. These are the first limits in the ZH channel based on Tevatron Run II data.

We thank the staffs at Fermilab and collaborating institutions, and acknowledge support from the DOE and NSF (USA); CEA and CNRS/IN2P3 (France); FASI, Rosatom and RFBR (Russia); CAPES, CNPq, FAPERJ, FAPESP, and FUNDUNESP (Brazil); DAE and DST (India); Colciencias (Colombia); CONACyT (Mexico); KRF and KOSEF (Korea); CONICET and UBACyT (Argentina); FOM (The Netherlands); PPARC (United Kingdom); MSMT (Czech Republic); CRC Program, CFI, NSERC, and WestGrid Project (Canada); BMBF and DFG (Germany); SFI (Ireland); The Swedish Research Council (Sweden); Research Corporation; Alexander von Humboldt Foundation; and the Marie Curie Program.

*On leave from IEP SAS Kosice, Slovakia.

†Visitor from Helsinki Institute of Physics, Helsinki, Finland.

- [1] S. Eidelman *et al.*, Phys. Lett. B **592**, 1 (2004); LEP Electroweak Working Group, <http://lepewwg.web.cern.ch/LEPEWWG/>.
- [2] M. Carena *et al.*, hep-ph/0010338.
- [3] L. Babukhadia *et al.*, Fermilab Report No. FERMILAB-PUB-03/320-E.
- [4] M.L. Ciccolini, S. Dittmaier, and M. Kramer, Phys. Rev. D **68**, 073003 (2003).
- [5] V. Abazov *et al.* (D0 Collaboration), Phys. Rev. Lett. **94**, 091802 (2005).
- [6] A. Abulencia *et al.* (CDF Collaboration), Phys. Rev. Lett. **96**, 081803 (2006).
- [7] V. Abazov *et al.* (D0 Collaboration), Nucl. Instrum. Methods Phys. Res., Sect. A (to be published).
- [8] S. Abachi *et al.*, Nucl. Instrum. Methods Phys. Res., Sect. A **338**, 185 (1994).
- [9] T. Sjöstrand *et al.* (PYTHIA Collaboration), Comput. Phys. Commun. **135**, 238 (2001).
- [10] M. Mangano *et al.* (ALPGEN Collaboration), J. High Energy Phys. 07 (2003) 1.
- [11] A. Pukhov *et al.* (COMPHEP Collaboration), hep-ph/9908288.
- [12] John Campbell and R.K. Ellis, Phys. Rev. D **65**, 113007 (2002); <http://mcfm.fnal.gov/>.
- [13] R. Brun and F. Carminati, CERN Program Library Long Writeup, Report No. W5013, 1993.
- [14] T. Junk, Nucl. Instrum. Methods Phys. Res., Sect. A **434**, 435 (1999); A. Read, CERN Report No. 2000-005, 2000.
- [15] D. Acosta *et al.* (CDF Collaboration), Phys. Rev. Lett. **95**, 051801 (2005).